Journal of
Composites Science

MDPI

Article

Effect of Nanostructured Silica Additives on the Extrusion-Based 3D Concrete Printing Application

Zhenbang Liu [1], Mingyang Li [1], Guo Sheng James Moo [2], Hitoshi Kobayashi [2], Teck Neng Wong [1] and Ming Jen Tan [1,*]

[1] Singapore Centre for 3D Printing, School of Mechanical & Aerospace Engineering, Nanyang Technological University, 50 Nanyang Avenue, Singapore 639798, Singapore; zhenbang001@e.ntu.edu.sg (Z.L.); limingyang@ntu.edu.sg (M.L.); mtnwong@ntu.edu.sg (T.N.W.)
[2] EVONIK (SEA) PTE. LTD., Asia Research Hub, 21 Biopolis Road, #01-35 Nucleos Tower A (South) Level 1M, Singapore 138567, Singapore; james.moo@evonik.com (G.S.J.M.); hitoshi.kobayashi@evonik.com (H.K.)
* Correspondence: mmjtan@ntu.edu.sg

Abstract: Recently, 3D printing technology has become more popular in the field of construction. For the extrusion-based 3D concrete printing (3DCP) process, the cementitious material needs to be strong and flowable enough to ensure buildability and pumpability. Nanostructured silica, a kind of additive, has been used to modify the 3DCP concrete to meet these requests. However, most previous studies focused on the effect of nanostructured silica on rheological properties and failed to link the obtained rheological properties of nanostructured-silica-modified cementitious materials to the performance in 3D printing. In this paper, the 3DCP mixture based on premix cement, river sand, silica fume, and water was modified by different dosages of nanostructured silica (from 0.25% to 1.00% by the total weight of the 3DCP mixture). The effects of nanostructured silica on the rheological, hydration, printing, and microstructural properties were determined by rheological tests, stress growth tests, setting time tests, printing tests, and scanning electron microscopy (SEM) tests, respectively. This paper revealed that the nanostructured silica has a positive effect on 3DCP buildability but negatively affects the printing quality, which fits the effect of nanostructured silica on the rheological properties. Hence, the determined rheological properties can qualitatively evaluate the printing performance of nanostructured-silica-modified cementitious materials.

Keywords: 3D concrete printing; additive manufacturing; nanostructured silica; buildability; scanning electron microscopy (SEM)

Citation: Liu, Z.; Li, M.; Moo, G.S.J.; Kobayashi, H.; Wong, T.N.; Tan, M.J. Effect of Nanostructured Silica Additives on the Extrusion-Based 3D Concrete Printing Application. *J. Compos. Sci.* **2023**, *7*, 191. https://doi.org/10.3390/jcs7050191

Academic Editors: Yan Zhuge, Zhenhua Duan and Wahid Ferdous

Received: 17 March 2023
Revised: 4 April 2023
Accepted: 5 May 2023
Published: 8 May 2023

1. Introduction

In the past few decades, 3D printing technology, regarded as additive manufacturing, has been widely used in the aerospace and biomedical fields [1,2]. Recently, it has become more popular in building and construction. One typical method is to combine traditional concrete-cast technology with 3D printing technology. As studied by Burger et al. [3] and Jipa et al. [4], non-cementitious material, such as polymers, is feasible to be printed as the formwork for cast concrete. In this system, the 3D printed formwork provides the possibility of a flexible design, and the cast concrete provides the loading resistance for structures. In addition to cementitious material as the loading-resistance material, it can also be acted as the material for 3D printing. The corresponding technology is called 3D concrete printing (3DCP). A series of projects, such as contouring crafting, D-shape project, and concrete printing, applied the 3DCP technology due to its high-level automation [5,6]. Among all methods in the 3DCP technology, the one which is most widely used is extrusion-based 3DCP [7], where the fresh state cementitious material is extruded layer by layer via a pumping system without any formwork [8]. Since the cost of formwork and corresponding labor accounts for a significant part of the total cost [9], the 3DCP can save the total cost of construction [10]. Additionally, same as the 3D printing technology in other fields, the

3DCP technology allows the flexible design for different-style structures, which can satisfy architectural requirements and reduce material waste [11,12].

Because of no formwork for extrusion-based 3DCP, the fresh cementitious material shall have enough strength and modulus to resist the increasing gravity and deformation during the printing process [13], which is regarded as buildability for 3D printing. On the other hand, due to the usage of the pumping system, the fresh cementitious material shall have enough workability to guarantee a smooth extrusion [14], which is regarded as pumpability for 3D printing. It is believed that the cementitious material which satisfies the requirement of buildability and pumpability tends to possess a high thixotropy, a material rheological property about the yield stress recovery and development [15,16]. Therefore, to obtain suitable material for 3D printing, different kinds of additives were applied to modify the rheological properties of fresh cementitious materials, such as accelerator, superplasticizer, nano-clay, and nanostructured silica. Among all additives, nanostructured silica shows great potential. The corresponding comparison can be summarized as follow. Even though Ramakrishnan et al. [17] reported that the encapsulated accelerator could improve 500% and 220% strength and modulus of 3D printed filament with excellent pumpability, it can lead to the rapid development of hydration temperature and shrinkage cracks [18]. Opposite to the accelerator, the effect of the superplasticizer is mainly to enhance material pumpability by reducing the dynamic yield stress [19]. However, at the same time, the static yield stress is negatively affected, which reduces the possibility of high buildability. Compared with the accelerator and superplasticizer, nano-particles, such as nanostructured silica and nano-clay, are not only effective in enhancing the static yield stress for 3DCP [20–23] but also provide better mechanical and durable performances [23,24]. The background mechanisms mainly contain three aspects based on Neville [18]: firstly, due to the significantly large surface area, nanostructured silica and nano-clay tend to absorb the free water, which can result in the enhancement of the yield stress; Secondly, the silicon dioxide (SiO_2) contained in nanostructured silica and nano-clay will react with $Ca(OH)_2$ and H_2O to produce C-S-H which is the main hydration product to provide strengths for cementitious materials (pozzolanic reaction); thus, mechanical properties of cementitious materials are improved by nanostructured silica and nano-clay. Thirdly, particles of nanostructured silica and nano-clay can easily fill in the pores among cement particles, which can result in the improvement of mechanical properties and durability for cementitious materials. Moreover, according to the studies conducted by [25–28], the mechanical performances of cementitious materials are enhanced with the increasing dosage of silicon dioxide (SiO_2). Thus, in the aspect of improving material mechanical properties, nanostructured silica possesses more potential compared with nano-clay. On the other hand, Reales et al. [21] demonstrated that nanostructured silica is a more effective inorganic thickener and accelerator to improve the initial value and growth rate of material static yield stress compared to nano-clay. Consequently, in the aspect of modifying the material rheological properties, nanostructured silica shows more potential as well.

Even though nanostructured silica shows more potential among additives, most studies focused on the effect of nanostructured silica on rheological properties and failed to link the effect of nanostructured silica on the rheological properties to the corresponding effect on the performance in real printing. To fill the research gaps, different dosages of nanostructured silica (from 0.25% to 1.00% by the total weight) were selected to study the effect of nanostructured silica on the rheological, hydration, printing, and microstructural properties by conducting rheological tests, stress growth tests, setting time tests, printing tests, and scanning electron microscopy (SEM) tests, respectively. By applying different failure criteria, this study established the link between the rheological properties and the 3DCP performance of nanostructured-silica-modified cementitious materials.

2. Materials and Methods

2.1. Methods

Based on the introduction in Section 1, most studies focused on the effect of nanostructured silica on the rheological properties of fresh cementitious materials; however, limited papers studied the link between the rheological properties and printing performances for nanostructured-silica-modified cementitious materials. Therefore, this study conducts the flow chart as shown in Figure 1. Firstly, the cementitious material, based on premix cement, sand, silica fume, and water, is modified by different dosages of solid powder and liquid aqueous dispersion nanostructured silica (from 0 to 1.00% by the weight of 3DCP mixture). Secondly, to study the effect of nanostructured silica on the rheological properties, hydration process, printing performances, and hydration products of 3DCP mixture, rheological tests, stress growth tests, setting time tests, printing tests, and SEM tests are conducted, respectively. Thirdly, by combining the analysis of rheological tests, stress growth tests, and setting time tests, the mechanism of the nanostructured silica affecting the rheological properties will be determined. Finally, by printing and SEM test results, the 3DCP performances will be evaluated by macro-scale printing characteristics and micro-scale hydration products. On the other hand, through different failure criteria, the rheological properties of nanostructured-silica-modified cementitious materials will be linked to the printing performances.

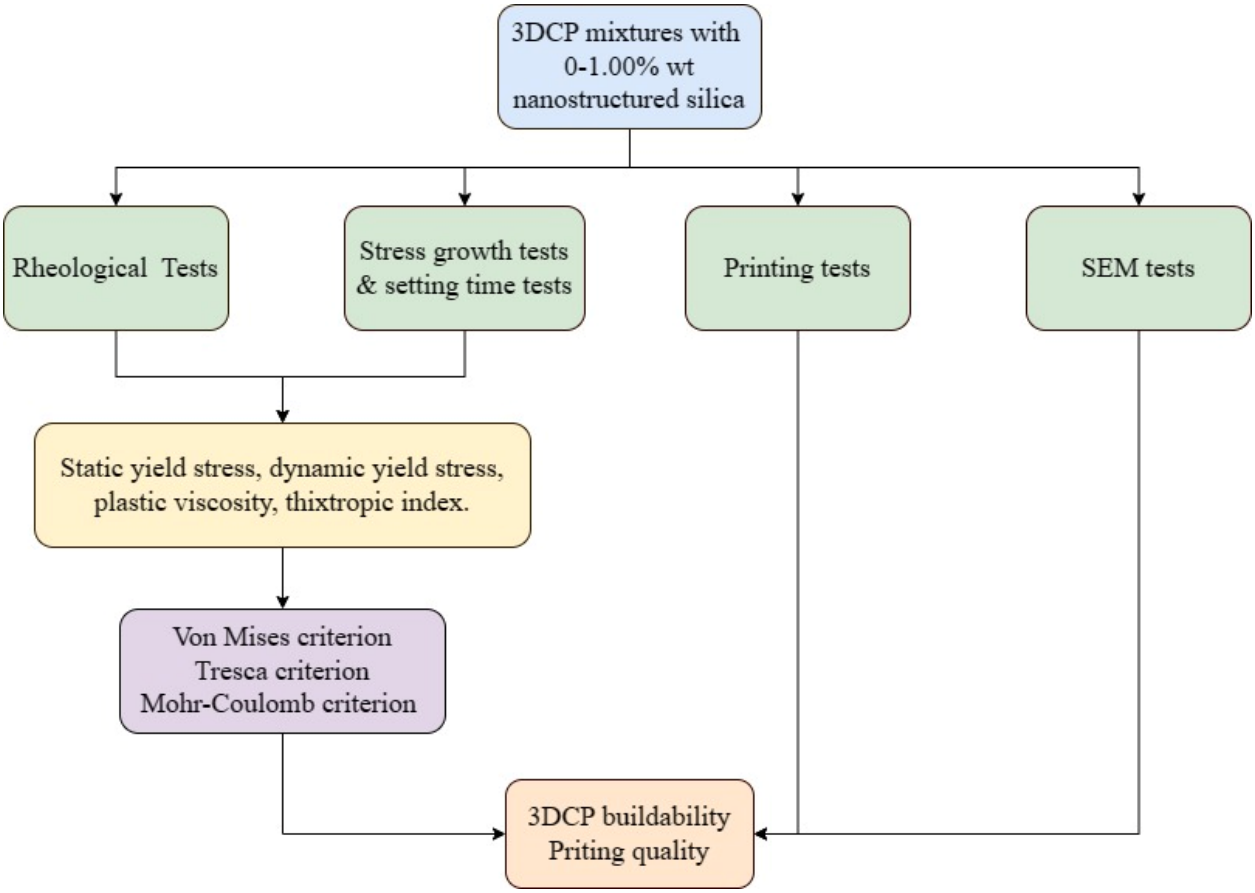

Figure 1. Flow chart in this paper to study the effect of nanostructured silica on 3D printing.

2.2. Material and Mixing Process

Synthetic amorphous silica (SAS) is an industrially produced silica with this randomized internal structure. These are produced commercially from processes such as fumed process and precipitation process. Commercial manufacturer, such as Evonik, produces all these grades in the category of SAS. In the fumed silica process, a precursor for the

silica is dosed into a hydrogen/oxygen flame, where the silica is formed at very high temperatures. Silica grades produced according to this process are called fumed silica. Evonik's brand name for fumed silica is AEROSIL®. (EVONIK (SEA) PTE. LTD, Singapore, Singapore) Liquid dispersion chemistry based on such fumed silica is produced under the AERODISP® (EVONIK (SEA) PTE. LTD, Singapore, Singapore). In the precipitated silica process, the silica is precipitated from an aqueous solution of waterglass. Silica produced by this process is called precipitated silica. Evonik's brand names for precipitated silica are SIPERNAT® (EVONIK (SEA) PTE. LTD, Singapore, Singapore). These materials are often nanostructured, with a nanoscale structure within the material or at its surface.

The 3DCP mixtures in this study consist of premix cement (PHOENIX Portland-Composite Cement—LAFARGE, Buildmate PTE. LTD, Singapore, Singapre), river sand (particle size $\leq$ 2 mm), silica fume (Microsilica Grade 940, Elkem company, Singapore, Singapore), water, solid powder nanostructured precipitated silica (SIPERNAT ® 380, EVONIK (SEA) PTE. LTD, Singapore, Singapore) or liquid aqueous dispersion of nanostructured fumed silica (AERODISP® W 7520 P, EVONIK (SEA) PTE. LTD, Singapore, Singapore), and tap water. The corresponding mixture compositions are presented in Table 1. The liquid aqueous dispersion of nanostructured silica is the solution containing 20% nanostructured silica powder by the total solution weight, and the corresponding composition also follows Table 1 after counting in the water in the liquid aqueous dispersion of nanostructured silica. The proportions of premix cement, river sand, silica fume, and water are the same among all mixtures. The mixture without nanostructured silica is considered the reference group (REF), and the other four mixtures contain different dosages of nanostructured silica from 0.25% to 1.00% by the weight of the REF.

Table 1. 3D concrete printing (3DCP) mixtures composition (kg/m^3).

Name of Mixture	Silica Type	Premix Cement	River Sand (0–2 mm)	Silica Fume	Water	Nanostructured Silica
REF	NA	1151.30	590.00	28.80	413.70	-
SIP380_0.25%	Solid	1151.30	590.00	28.80	413.70	5.46
SIP380_0.50%	Solid	1151.30	590.00	28.80	413.70	10.92
SIP380_0.75%	Solid	1151.30	590.00	28.80	413.70	16.38
SIP380_1.00%	Solid	1151.30	590.00	28.80	413.70	21.84
W7520P_0.25%	Liquid	1151.30	590.00	28.80	413.70	5.46
W7520P_0.50%	Liquid	1151.30	590.00	28.80	413.70	10.92
W7520P_0.75%	Liquid	1151.30	590.00	28.80	413.70	16.38
W7520P_1.00%	Liquid	1151.30	590.00	28.80	413.70	21.84

Table 2. Mixing process.

Mixing Time (min)	Rotational Speed (rpm)	Solid Powder Case	The Liquid Aqueous Dispersion of Nanostructured Silica Case
0.5	33	Sand + nanostructured silica	Sand
0.5	61	-	-
0.5	33	Premix cement + silica fume	Premix cement + silica fume
0.5	61	-	-
1.0	33	Water	Water + nanostructured silica
0.5	61	-	-
1.0	113	-	-

Hobart Mixer HL200 was applied for the material mixing. The mixing process is shown in Table 2. For the solid powder nanostructured silica case, firstly, the powders of sand and solid powder nanostructured silica are mixed at 33 rpm for 0.5 min and 61 rpm

for 0.5 min. Secondly, premix cement and silica fume are added and mixed at 33 rpm for 0.5 min and 61 rpm for 0.5 min. Thirdly, water is added to the mixer with the rotational speed at 33 rpm for 0.5 min. Finally, the mixing procedure continues at 61 rpm for 0.5 min and 113 rpm for 1 min. For the liquid aqueous dispersion of the nanostructured silica case, the liquid aqueous dispersion of nanostructured silica is added to water, and the corresponding solution is mixed with all powders in the third step.

2.3. Experimental Design

Since the properties of fresh cementitious material are significantly affected by the environmental temperature and moisture [16], the rheological test, shear stress test, setting time test, and printing test were conducted in the laboratory with the temperature and humidity at 22.5 °C and 56%, respectively.

2.3.1. Rheological Test

In the 3DCP process, the cementitious material is extruded layer by layer through the pumping system without any formwork support. Thus, the fresh cementitious material is required to possess enough buildability and pumpability to resist the increasing gravity and smoothly flow through the pumping system. It is believed that the buildable and pumpable cementitious material has a high thixotropy, a rheological property correlated to the material yield stress and plastic viscosity [15,16].

In this part, a Schleibinger Viskomat XL rheometer with 10,000 N·mm maximum torque was used as the test device, with the rotational speed and torque recorded once per second. A rheological test protocol (Figure 2a), based on Weng et al. [14], was applied to determine the effect of nanostructured silica on the static yield stress, dynamic yield stress, and plastic viscosity, which contains two stages. Firstly, the rotational speed of the rheometer stirrer linearly increases from 0 rpm to 60 rpm within 5 min. In this stage, the peak value of torque (Figure 2b), regarded as the static torque, can be converted into the material static yield stress by Equation (1). [29]. Secondly, the rotational speed of the rheometer stirrer linearly decreases from 60 rpm to 0 rpm in another 5 min. In this stage, the torque viscosity and flow resistance (Figure 2b) can be converted into the dynamic yield stress and plastic viscosity by Equation (2) since the rheological properties of fresh cementitious materials can be described by the Bingham model as Equation (3) [30].

$$\tau = \frac{T}{(2\pi {r_1}^3)\left(\frac{l}{r_1} + \frac{2}{3}\right)} \tag{1}$$

$$T = \frac{4\pi r_1^2 r_2^2 l \mu}{r_2^1 - r_2^1}\omega - \frac{4\pi r_1^2 r_2^2 l \tau_d}{r_2^1 - r_2^1} ln\frac{r_1}{r_2} \tag{2}$$

$$\tau = \tau_d + \mu\dot{\gamma} \tag{3}$$

where T (N·m) is the torque from the rheometer. τ (Pa) and τ_d (Pa) correspond to the shear stress and dynamic yield stress. μ (Pa·s) and $\dot{\gamma}$ (s^{-1}) represent the plastic viscosity and shear strain rate. ω (rad/s) is the rotational speed from the rheometer. r_1 (m) and l (m) are the radium and height of the rheometer stirrer, while r_2 (m) is the radium of the unit cell of the rheometer.

Furthermore, to study the effect of nanostructured silica on the material thixotropy, the thixotropic index (I_{thix}) was applied as Equation (4), based on Weng et al. [16].

$$I_{thix} = \frac{\tau_s}{\tau_d} \tag{4}$$

where τ_s (Pa) and τ_d (Pa) correspond to the material static yield stress and dynamic yield stress.

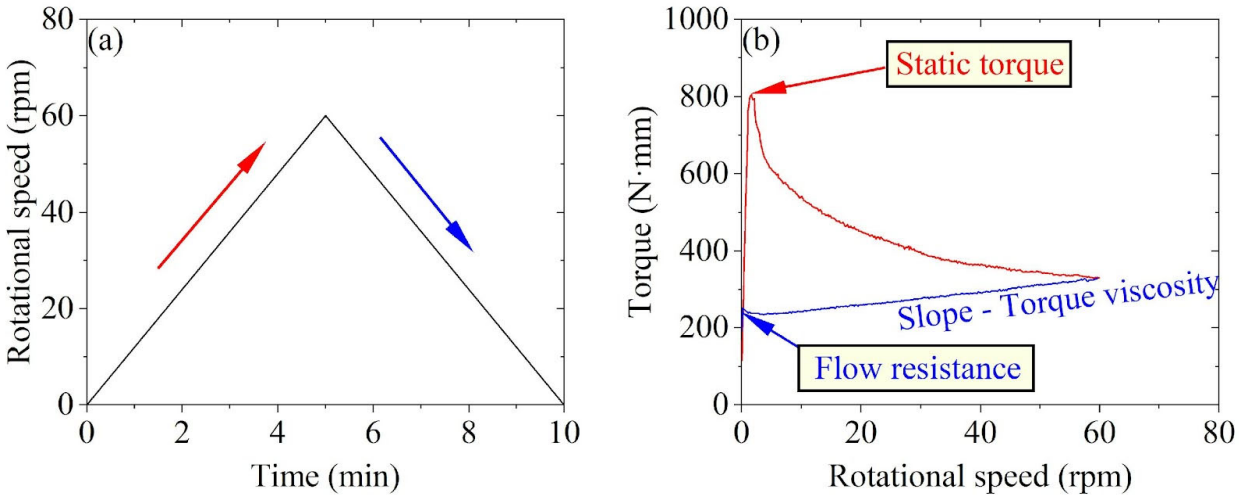

Figure 2. Rheological tests: (**a**) test protocol; (**b**) expected results.

2.3.2. Stress Growth Test

For 3DCP cementitious materials, the rheological properties are time-dependent. After the material is extruded from the pumping system, the material is under a resting state without shearing. During this period, the microstructure of the material tends to recover to the original state before shearing and continues to grow due to the flocculation and C-S-H nucleation [31]. Furthermore, as studied by Roussel [32], the relationship between the material static yield stress and the resting time can be modeled by Equation (5) as follows:

$$\tau_s = A_{\text{thix}} t + \tau_{s,\text{ini}} \quad (5)$$

where τ_s (Pa) is the static yield stress at a certain time, t (min), while A_{thix} (Pa/min) and $\tau_{s,\text{ini}}$ (Pa) are the growth rate and initial value of the static yield stress.

In this part, the effect of nanostructured silica on the growth pattern of the material static yield stress was studied to represent that on the growth pattern of the material rheological properties. An Anton Paar Modular Compact Rheometer (MCR 102) with 200 N·mm maximum torque and the stirrer of ST22-4V-16 was used as the test device, with the shear strain and torque recorded twice per second. A stress growth test protocol (Figure 3a) based on Kruger et al. [15] was applied to determine the material static yield stress. During the protocol, the shear strain rate was set as 0.1 s^{-1} for 2 min to avoid aggregate mitigation [33], and the static yield stress (Figure 3b) can be obtained by torque from Equation (1). Furthermore, to determine the evolution of the static yield stress, the stress growth test protocol, as mentioned above, was repeated at 0 min, 7 min, 14 min, 21 min, 28 min, and 35 min, respectively.

2.3.3. Setting Time

Compared with silica fume, nanostructured silica is much more active due to the large surface area; thus, it tends to positively affect the fresh cementitious material strength growth by accelerating the hydration of cementitious materials. To quantitively measure the effect of nanostructured silica on the hydration process, the setting time tests were conducted by using a MATEST VICAT apparatus. In these setting time tests, the needle of the VICAT apparatus was set to penetrate the material 41 times with 10 min time intervals, according to ASTM C191 [34]. Accordingly, the initial setting time can be estimated to the nearest 1 min based on Equation (6)

$$T_{setting} = \left(\left(\frac{H - E}{C - D} \right) \times (C - 25) \right) + E \quad (6)$$

where E (min) is the time of the last penetration higher than 25 mm, while C (mm) is the penetration depth at time E (min). H (min) is the time of the first penetration lower than 25 mm, while D (mm) is the penetration depth at time H (min).

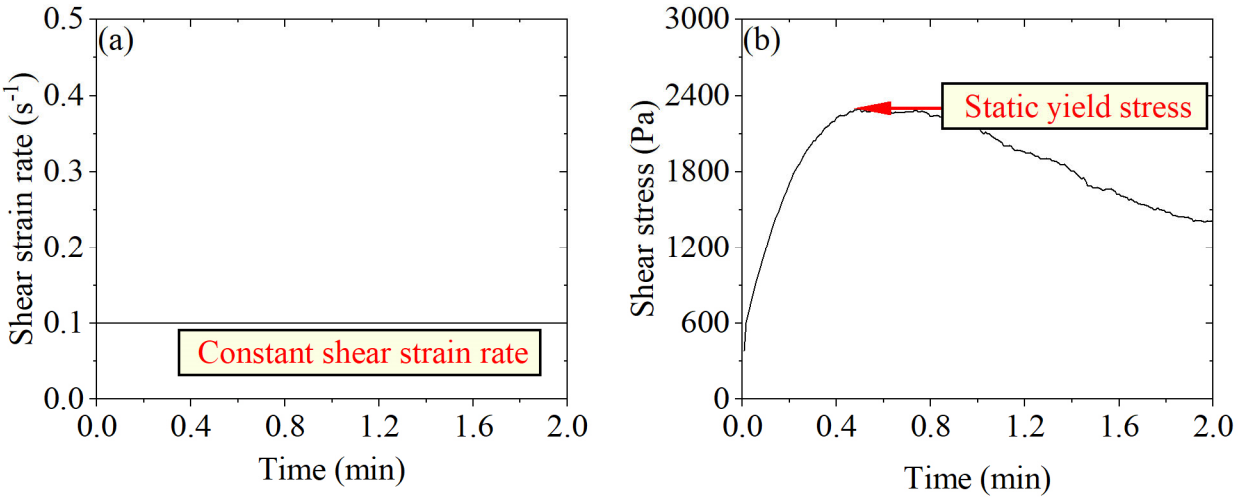

Figure 3. Stress growth tests: (**a**) test protocol; (**b**) expected results.

2.3.4. Printing Test

To investigate the effect of nanostructured silica on the performance in 3D printing, a series of printing tests were conducted via a customized printing system (in Figure 4), which includes a gantry printer with a 1.2 m × 1.2 m × 1.0 m ($L \times W \times H$) printing volume, an MAI Pictor pump, and a hose with 3 m in length and 2.54 cm in diameter. The printing path is a hollow circular column with a 100 mm inner diameter. The dimension of each filament was set as 20 mm in width and 10 mm in height. During the printing process, the pumping flow rate was 1.8 L/min, and the nozzle travel speed was 150 mm/s.

The whole printing test contains two rounds. The first round aimed to study the effect of nanostructured silica on buildability; thus, the printing process stopped till the printing sample collapsed. Correspondingly, when the final collapse happens, the maximum gravity-induced vertical stress (GIVS) can be calculated as follows:

$$\sigma_u = \rho g h \tag{7}$$

where σ_u (Pa) and h (m) are maximum gravity-induced vertical stress (GIVS) and the printing height when the final collapse happens. ρ (kg/m^3) is the material density. The second round of printing tests aimed to study the effect of nanostructured silica on the material pumpability and printing quality; thus, the printing process stopped until the cylinder column achieved $x - 1$ layers, with x equal to the maximum layers in the first-round printing.

2.3.5. Scanning Electron Microscopy (SEM) Analysis

To study the effect of nanostructured silica on the hydration products of the 3DCP cementitious material. A series of scanning electron microscopy tests (SEM) was carried out, which includes solid powder nanostructured silica particles, liquid aqueous dispersion of nanostructured silica particles, the powder mixture of solid powder NS_1.00%, 28-day-water-cured REF 3DCP samples, 28-day-water-cured solid powder NS_1.00% 3DCP samples, and 28-day-water-cured liquid aqueous dispersion NS_0.75% 3DCP samples. Before SEM tests, all samples were coated with platinum under 30 mA currents for 15 s. Then, the samples were scanned by FE-SEM device: JEOLJSM-6340F. The accelerating voltage and probe current of FE-SEM 6340F were set as 5 kV and 12 μA, respectively.

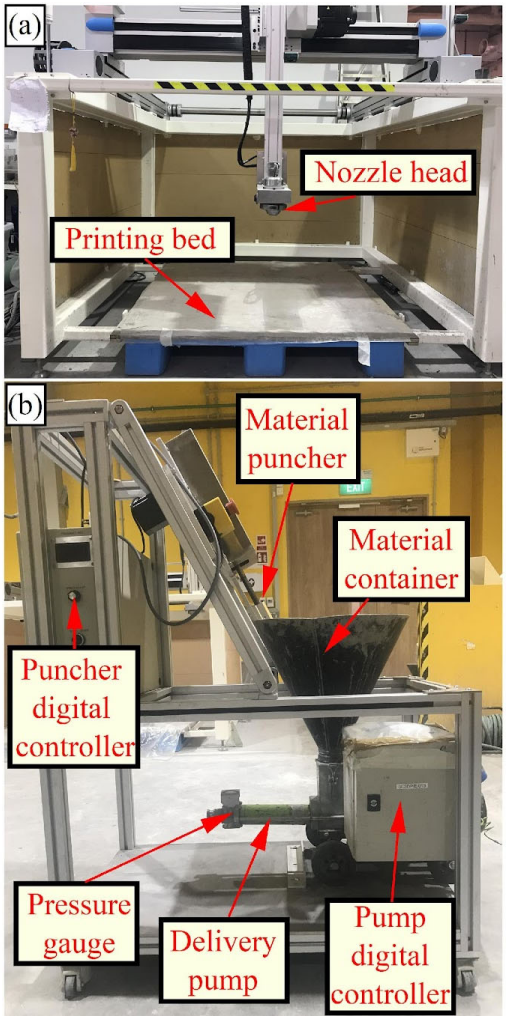

Figure 4. (**a**) Gantry 3DCP Printer; (**b**) pumping system for printing test.

3. Results and Discussion

3.1. Rheological Test Results

During the mixing process, it was observed that the workability of the cementitious material became worse with the increasing dosage of nanostructured silica. As shown in Figure 5, the mixture of aqueous dispersion NS_1.00% agglomerated after mixing and trapped the rheometer probe. Furthermore, the corresponding static yield stress is so high that it has been beyond the capacity of the rheometer. Thus, for W7520P_1.00%, the rheological properties and printing performances cannot be determined.

Except for W7520P_1.00%, the rheological test results of the remaining mixtures are shown in Figure 6, which include static yield stress, dynamic yield stress, plastic viscosity, and thixotropy index. Firstly, from Figure 6a, it can be observed that as the dosage of solid powder nanostructured silica increases from 0% to 1.00%, the static yield stress tends to increase significantly from 1110 Pa to 3942 Pa, and for the liquid aqueous dispersion of nanostructured silica cases, the static yield stress increases from 1110 Pa for REF to 4388 Pa for W7520P_0.75%. The significant enhancement of static yield stress can be attributed to the enormous surface area of nanostructured silica particles absorbing the free water [35]. Hence, nanostructured silica can be considered an inorganic viscosity-modifying admixture (VMA) and thickener [36]. Secondly, as shown in Figure 6b, the REF mixture without nanostructured silica possesses a 173 Pa dynamic yield stress. As the dosage of nanostructured silica increases from 0.25% to 0.75%, the dynamic yield stress slightly increases from 210 Pa to 290 Pa for solid powder nanostructured silica cases, while

the dynamic yield stress of liquid aqueous dispersion of nanostructured silica cases stays at approximately 230 Pa. Furthermore, with 0.25% more nanostructured silica application, the dynamic yield stress of solid powder nanostructured silica cases has a significant increase from 222 Pa to 428 Pa, and the dynamic yield stress of liquid aqueous dispersion of nanostructured silica cases cannot be determined due to the limitation of rheometer capacity. Thus, the dosage of 0.75% can be regarded as a threshold of nanostructured silica significantly affecting the material dynamic yield stress. Thirdly, from Figure 6(c), it can be observed that the plastic viscosity is not always increasing with more dosage of nanostructured silica. Instead, both solid powder nanostructured silica cases and liquid aqueous dispersion nanostructured silica cases achieve their peak plastic viscosity at the dosage of 0.75%. Finally, as shown in Figure 6d, the effect of nanostructured silica on the material thixotropic index has a similar trend as the one of plastic viscosity. Thus, to obtain the cementitious material with the highest thixotropy, the optimal dosage of nanostructured silica shall be 0.75% by the total weight of the 3DCP mixture.

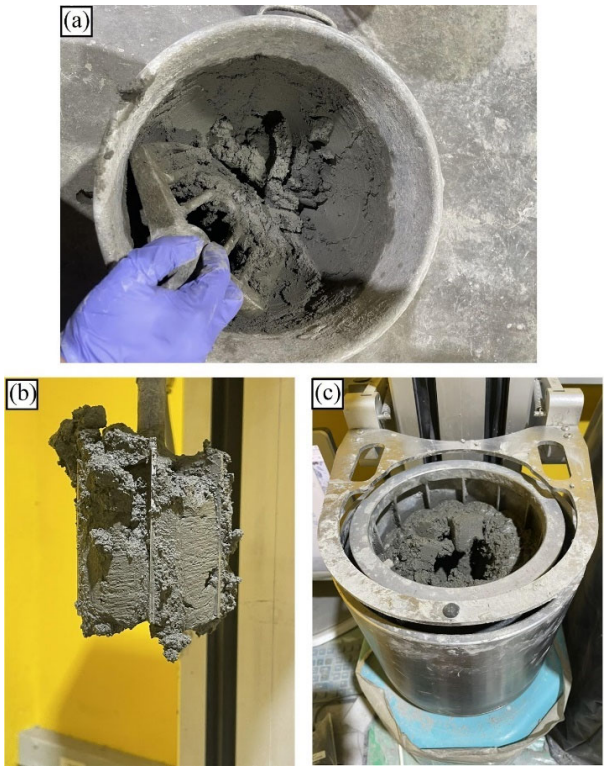

Figure 5. The workability of liquid aqueous dispersion NS_1.00%: (**a**) the state of the mixture after mixing; (**b**) the state of the rheometer probe; (**c**) the state of the mixture in the unit cell.

3.2. Stress Growth Test Results

The effects of nanostructured silica on the growth pattern of the material rheological properties were represented by the effect of nanostructured silica on the growth pattern of the static yield stress. As shown in Figure 7, the development of the static yield stress of REF and nanostructured-silica-modified 3DCP materials can be approximately described by linear fitting, which is summarized in Table 3. By combining Figure 7 and Table 3, it is evident that the 3DCP material without nanostructured silica achieves the lowest R^2 value as 0.7873, while the growth of the static yield stress of the nanostructured-silica-modified is more closed to the straight line, which is consistent with the model of Roussel [37]. Moreover, the solid powder nanostructured silica and liquid aqueous dispersion nanostructured silica show similar effects on enhancing the initial value and growth rate of the static yield stress. As the dosage of solid powder nanostructured silica increases from 0% to 1.00%, the initial value of the static yield stress increase from 821 Pa to 3988 Pa, and the growth rate of the static yield stress is improved from 38 Pa/min to 68 Pa/min. On the other hand, as the

dosage of liquid aqueous dispersion nanostructured silica increases from 0% to 0.75%, the initial value of the static yield stress increase from 821 Pa to 3822 Pa, and the growth rate of the static yield stress is improved from 38 Pa/min to 65 Pa/min. Due to the enhancement of initial value and growth rate of the static yield stress, the nanostructured silica can improve both flocculation or C-S-H nucleation in fresh cementitious materials. Consequently, nanostructured silica can be regarded as an inorganic thickener or accelerator, which fits the conclusion of Lavergne et al. [22].

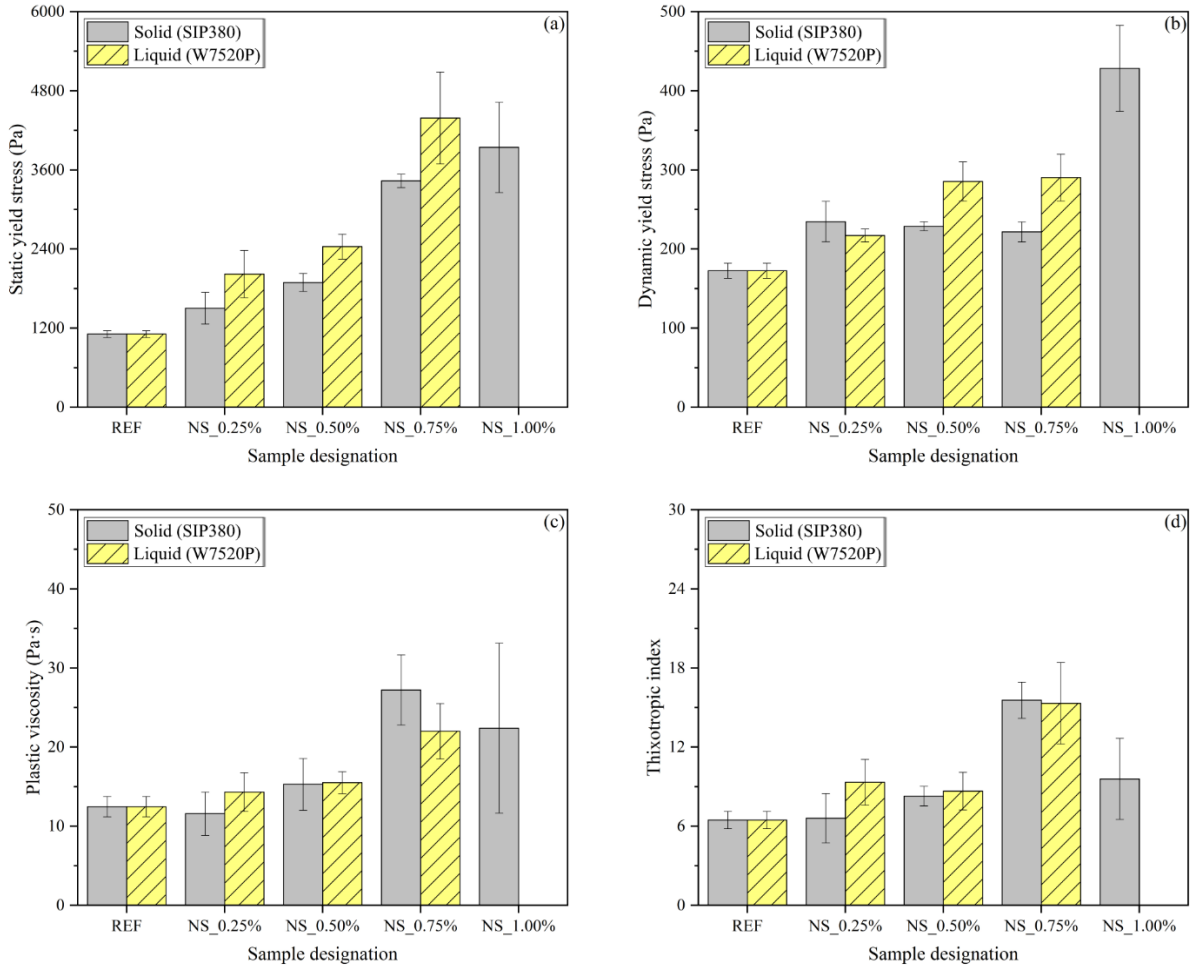

Figure 6. Rheological test results: (**a**) static yield stress; (**b**) dynamic yield stress; (**c**) plastic viscosity; (**d**) thixotropy index.

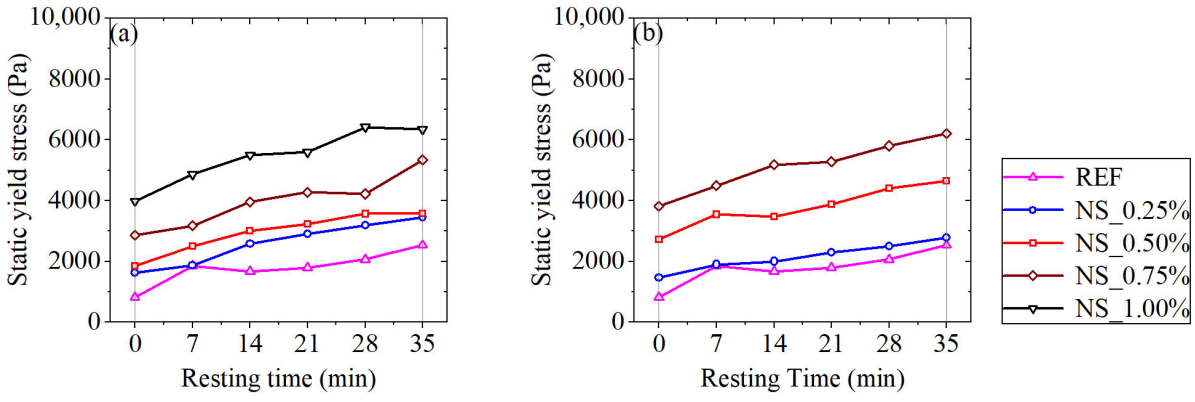

Figure 7. The evolution of static yield stress: (**a**) solid powder nanostructured silica cases; (**b**) liquid aqueous dispersion of nanostructured silica cases.

Table 3. The evolution of static yield stress (Pa) as the resting time (min).

Mixture	Static Yield Stress	R^2
REF	$\tau_s = 38t + 1122$	0.7873
SIP380_0.25%	$\tau_s = 55t + 1643$	0.9736
SIP380_0.50%	$\tau_s = 49t + 2094$	0.9168
SIP380_0.75%	$\tau_s = 65t + 2838$	0.9232
SIP380_1.00%	$\tau_s = 68t + 4274$	0.9209
W7520P_0.25%	$\tau_s = 35t + 1537$	0.9795
W7520P_0.50%	$\tau_s = 52t + 2877$	0.9392
W7520P_0.75%	$\tau_s = 65t + 3989$	0.9687
W7520P_1.00%	NA	NA

3.3. Setting Time Results

As discussed in stress growth tests, the nanostructured silica improves the growth rate of the static yield stress. To study the mechanism of enhancing the static yield stress development, setting time tests were conducted. As shown in Figure 8, with the increasing dosage of nanostructured silica, the initial setting time of cementitious materials tends to decrease (from 202 min to 105 min for solid powder nanostructured silica cases and 202 min to 153 min for liquid aqueous dispersion nanostructured silica cases); however, the decreasing trend of the initial setting time becomes slower, which is consistent with the test results of Sikora et al. [38]. Hence, the effect of nanostructured silica on the enhancement of static yield stress evolution is attributed to nanostructured silica improving the hydration process, and nanostructured silica can be considered an inorganic accelerator. However, the corresponding effect as an accelerator tends to be more insignificant with the increasing dosage of nanostructured silica.

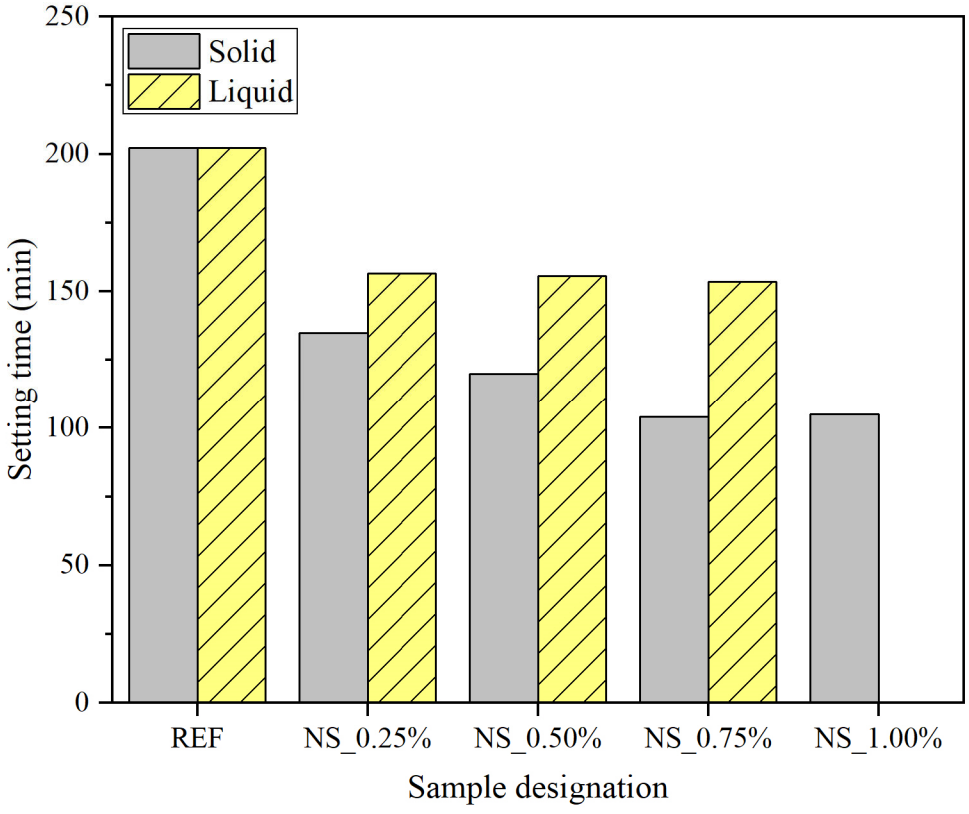

Figure 8. Initial setting time.

3.4. Printing Test Results

To study the effect of nanostructured silica on the 3DCP performance, the modified cementitious materials were printed for two rounds, as shown in Figures 9 and 10.

Figure 9. *Cont.*

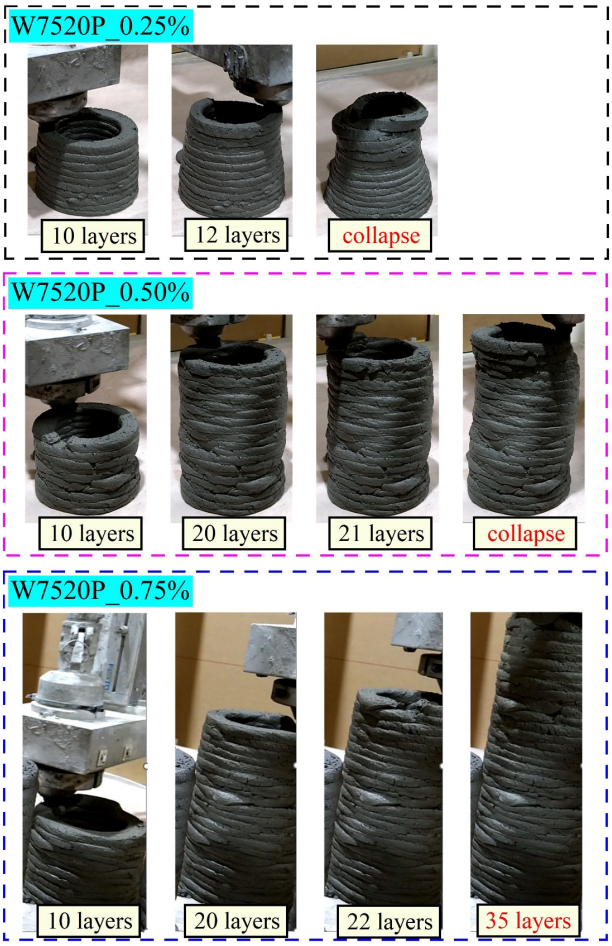

Figure 9. The printing test results of the first round.

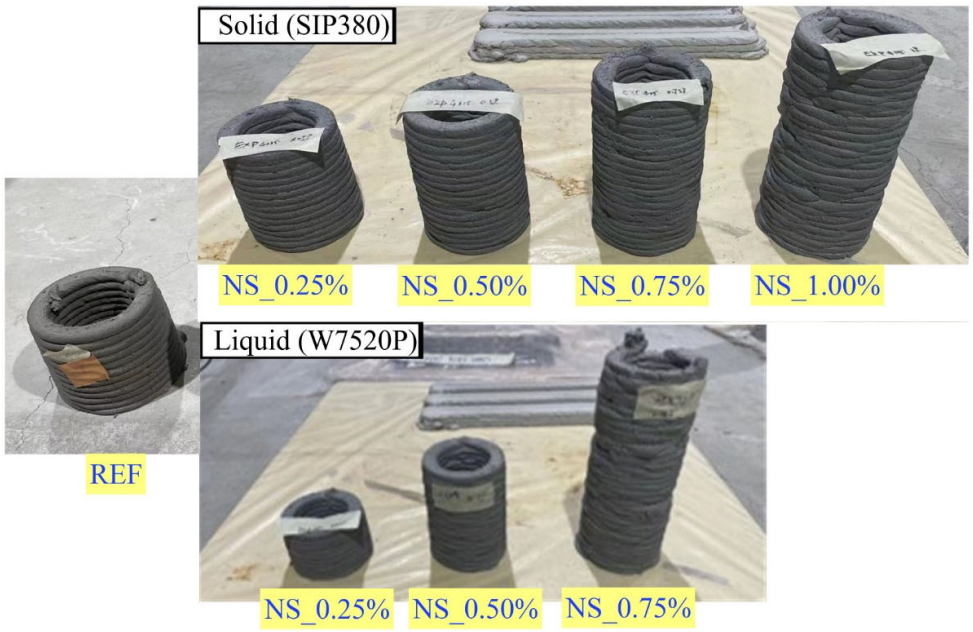

Figure 10. Printed samples after the second-round printing.

As the aspect of the printing quality, it can be observed that For REF and liquid aqueous dispersion NS_0.25%, the materials are printed smoothly without any cracks or discontinuity. The deformation of the printed samples continuously develops until the

cylinder collapses at the 13th layer and 12th layer extrusion, and it is difficult to determine the exact position where the deformation happens. Thus, 0.25% liquid aqueous dispersion nanostructured silica does not significantly affect the printing quality. For solid powder NS_0.25%, there is no obvious deformation for the first 10-layer printing; however, apparent deformation can be observed when the material is printed till the 16th layer extrusion, and the deformation continues to develop until the cylinder collapse at the 18th layer extrusion. For solid powder NS_0.50%, no apparent deformation can be observed; however, continuous cracks appear at the final stage of the printing (20th layer extrusion). For solid powder NS_0.75%, solid powder NS_1.00%, liquid aqueous dispersion NS_0.50%, and liquid aqueous dispersion NS_0.75%, cracks and discontinuity exist during the whole printing process. The cracks and discontinuity become more significant as the increasing dosage of nanostructured silica. Therefore, it indicates that the nanostructured silica tends to negatively affect the printing quality, which is consistent with the effect of nanostructured silica on the material dynamic yield stress.

In addition to the printing quality, the effect of nanostructured silica on buildability is described by the maximum gravity-induced vertical stress (GIVS) of 3DCP, based on Equation (7). As shown in Figure 11, it can be observed that for solid powder nanostructured silica cases, as the dosage of nanostructured silica increases from 0% to 1.00%, the maximum GIVS tends to increase from 2678 Pa to 5768 Pa linearly. Different from solid powder nanostructured silica cases, 0.25% liquid aqueous dispersion nanostructured silica shows a significant influence on the maximum GIVS; however, when the nanostructured silica is beyond 0.25%, the maximum GIVS significantly increases to 4120 Pa for liquid aqueous dispersion NS_0.50% and 7416 Pa for liquid aqueous dispersion NS_0.75%. Consequently, it suggests that the nanostructured silica tends to benefit the buildability, which fits the effect of nanostructured silica on the static yield stress. The effect of liquid aqueous dispersion nanostructured silica on the 3DCP buildability tends to be more effective than the one of solid powder nanostructured silica, which can be attributed to more uniform particle distribution for the liquid aqueous dispersion of nanostructured silica case and can also be related to different particle sizes for these two types of nanostructured silica.

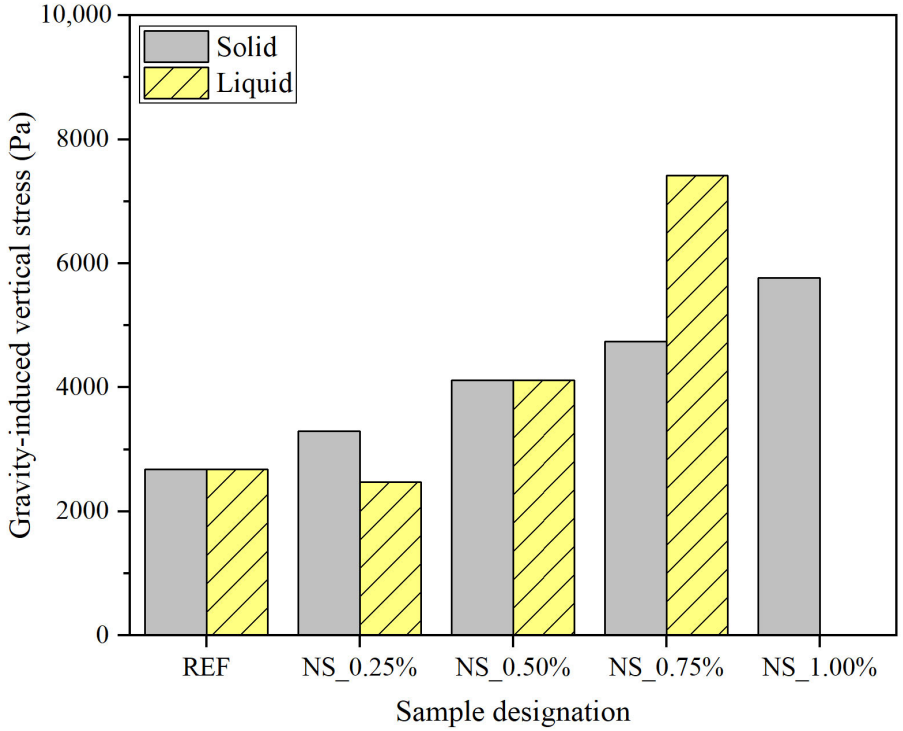

Figure 11. The maximum gravity-induced vertical stress (GIVS) in the first-round printing.

Therefore, the printing tests indicate that nanostructured silica benefits the material buildability and negatively affects the printing quality, which is consistent with the effect of nanostructured silica on the rheological properties. In the next step, the effect of nanostructured silica on rheological properties will be quantitatively compared with the corresponding effect on the printing performances.

3.5. Comparison of Different Test Results

In this part, the relationship between the compressive strength and shear strength of fresh cementitious material is applied to quantitatively compare the effect of nanostructured silica on the rheological properties and printing performance. As Roussel [25], the ratio of compressive strength and shear strength is equal to $\sqrt{3}$, based on the Von Mises failure criterion, while Kruger et al. [39] proposed that the corresponding ratio shall be equal to $2F_{AR}$ with F_{AR} as the confinement-related correction factor depending on the aspect ratio of filament cross-section, according to Tresca failure criterion. In addition, since the mechanism of fresh concrete to resist gravity is considered the same as cohesive soils [40], the Mohr–Coulomb failure criterion is available to describe the relationship between shear and compressive strength [41], which can be written as:

$$\tau_s = c = \frac{\sigma_u}{2}\cos\varphi - \frac{\sigma_u}{2}(1-\sin\varphi)\tan\varphi \quad (8)$$

where c (Pa) is the cohesion, and φ is the friction angle.

With the assumption that the period of the 3D printing process is negligible, the static yield stress from rheological tests, maximum gravity-induced vertical stress, and friction angle are compared in Table 4. It can be observed that as the dosage of nanostructured silica increases, the ratio of the maximum GIVS to static yield stress is not a constant but has a roughly decreasing tendency, which is not consistent with the model proposed by Roussel [32] and Kruger et al. [39]. It is because both Von Mises and Tresca failure criteria are valid for ductile materials instead of brittle cementitious materials. Additionally, it can be observed that except for REF, SIP380_0.25%, and SIP380_0.50%, the friction angles of each case are negative, which does not fit the domain of the friction angle and is not consistent with the test results of Li et al. [42]. The background reason can be that the maximum gravity-induced vertical stress from the printing tests underestimates the compressive strength of the fresh nanostructured-modified cementitious materials. As discussed in rheological tests, stress growth tests, and printing tests, nanostructured silica tends to benefit the buildability in 3DCP by enhancing the initial and growth rate of the static yield stress; however, the 3DCP buildability can also be affected by the printing quality, which is negatively influenced by the increasing usage of nanostructured silica.

Table 4. The relationship between static yield stress and maximum GIVS.

Mixture	τ_s	σ_u (Pa)	σ_u/τ_s	φ (°)
REF	1110	2678	2.41	10.68
SIP380_0.25%	1503	3296	2.19	5.27
SIP380_0.50%	1893	4120	2.18	4.84
SIP380_0.75%	3233	4738	1.47	<0
SIP380_1.00%	3942	5768	1.46	<0
W7520P_0.25%	2021	2472	1.22	<0
W7520P_0.50%	2437	4120	1.69	<0
W7520P_0.75%	4388	7416	1.69	<0
W7520P_1.00%	-	-	-	-

Consequently, it indicates that there is no optimal failure criterion to link the rheological properties to the corresponding printing performances; however, the rheological tests are still effective in qualitatively evaluating the printing performances for the

nanostructured-silica-modified cementitious materials. Additionally, to further determine the exact printing performances, the printing tests are essential to be conducted.

3.6. Scanning Electron Microscopy (SEM) Analysis Results

The effect of nanostructured silica on the hydration products of the 3DCP mixture is studied by SEM tests, as shown in Figures 12 and 13. For the pure nanostructured particle in Figure 12, it can be observed that both solid powder and solute nanostructured silica are spherical in shape, which is like fly ash and silica fume; however, the particle size of nanostructured is even smaller than 100 nm. Due to the extremely fine particle, nanostructured silica tends to be significantly active in improving the hydration kinetics as an inorganic accelerator [22]. For the REF and nanostructured-silica-modified silica in Figure 13, it can be observed that the printed sample of REF has incompletely unreacted fly ash and CH, indicating that the fly ash is not active enough to react with CH for the pozzolanic reaction. The remaining CH in REF suggests that the corresponding microstructure is dense sufficient to avoid carbonation. The SEM image of Solid powder NS_1.00% in Figure 13 shows that the hydration products mainly consist of C-S-H and ettringite. Compared with REF, it demonstrates that the CH has been reacted with nanostructured silica and converted into C-S-H through the pozzolanic reaction; however, the solid power NS_1.00% can be observed as much more porous, which reveals the negative effect of nanostructured silica on the printing quality. Different from the solid powder NS_1.00%, the SEM image of Liquid aqueous dispersion NS_0.75% in Figure 13 shows that its hydration products contain a cubic crystal layer. Due to the existence of ettringite in hydration products, the reactants of the hydration possess enough gypsum. Thus, the observed crystal layer is $CaCO_3$ instead of the hydrogarnet. Therefore, it indicates that the negative effect of liquid aqueous dispersion nanostructured silica is much more significant since the CO_2 in the air has permeated and converted CH into $CaCO_3$. Consequently, the effect of nanostructured silica on the printing performance can also be demonstrated by the hydration products of the 3DCP mixtures.

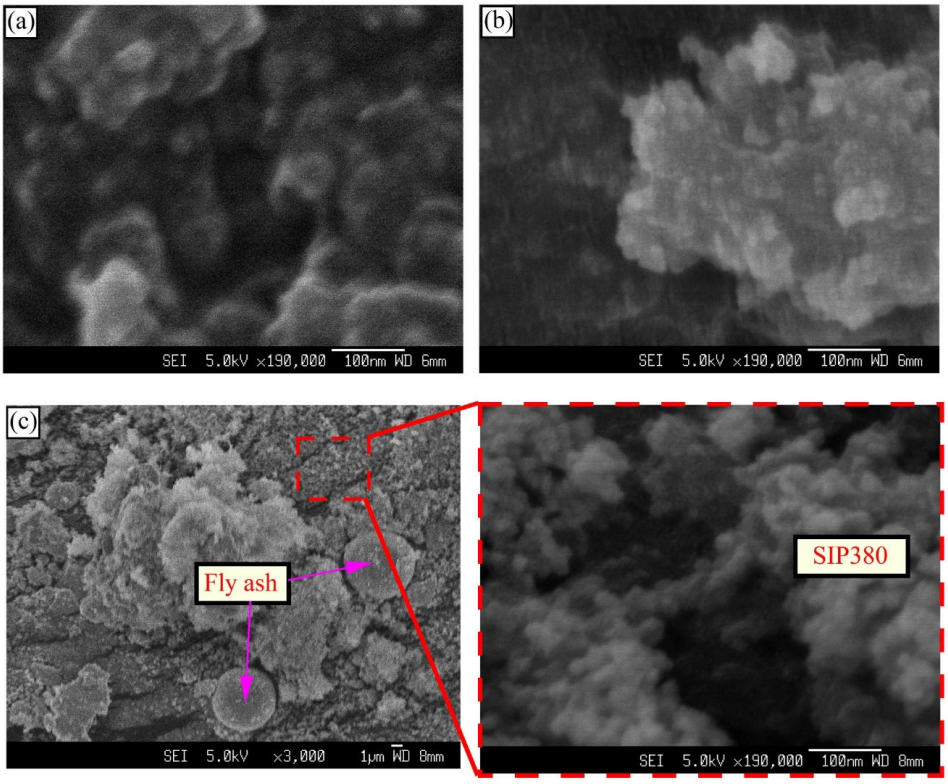

Figure 12. SEM images: (**a**) Solid powder nanostructured silica powder; (**b**) the solute of liquid aqueous dispersion nanostructured silica; (**c**) the powder mixture of solid powder NS_1.00%.

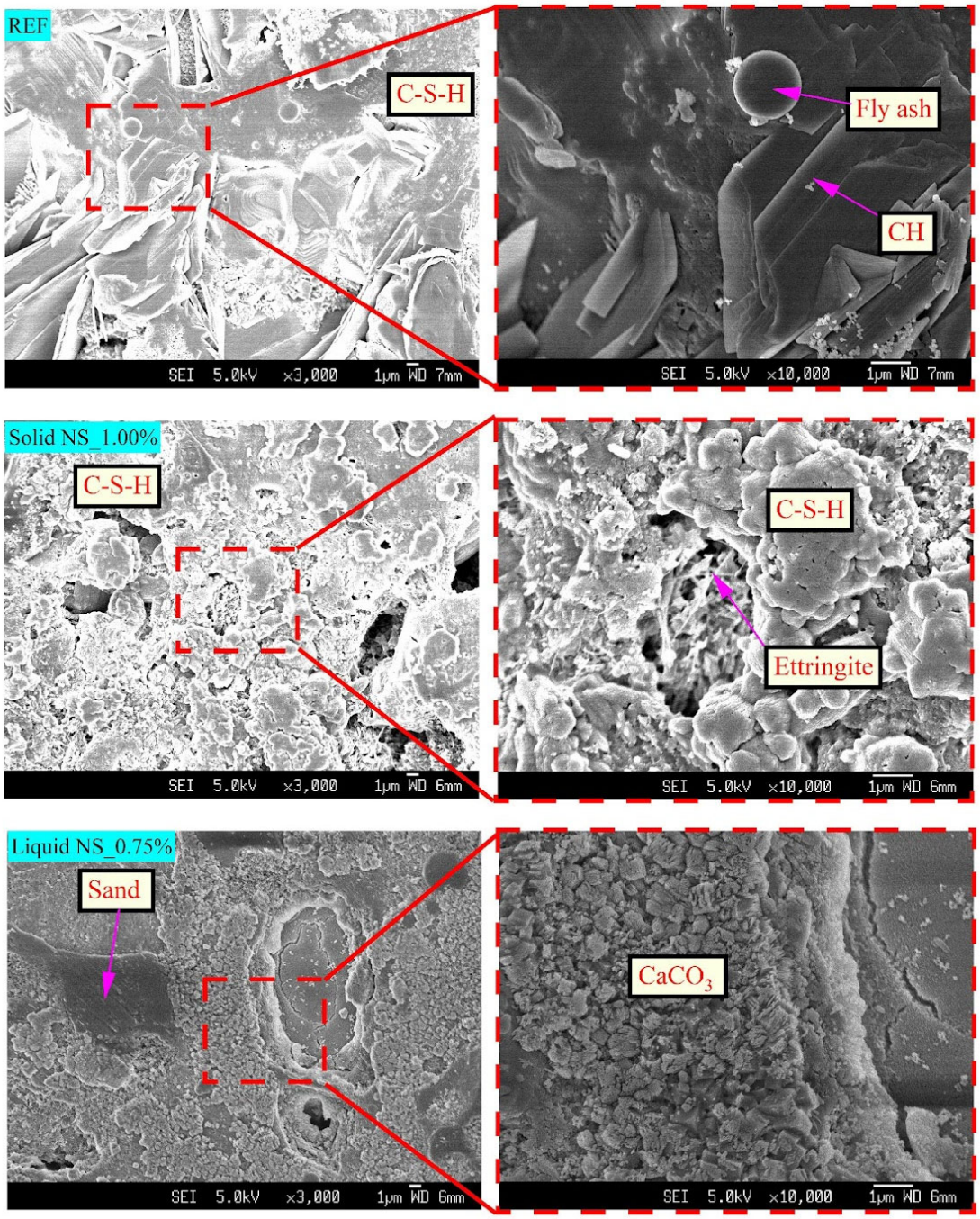

Figure 13. SEM images of REF, solid powder NS_1.00%, and liquid aqueous dispersion NS_0.75%.

4. Conclusions

In this paper, a series of experiments have been conducted to study the effect of solid powder and liquid aqueous dispersion nanostructured silica on the properties of 3D printing cementitious materials. The corresponding conclusions can be drawn as follows:

1. Through rheological tests, it confirms that the nanostructured silica tends to improve the static yield stress, dynamic yield stress, and plastic viscosity. To determine the fresh cementitious material with the highest thixotropy, the optimal dosage of nanostructured silica is 0.75% by the weight of the total 3DCP mixture.
2. Stress growth tests demonstrate that nanostructured silica has similar effects as an organic thickener and accelerator since it improves the initial value and growth rate of

the static yield stress. Its corresponding effect on accelerating hydration is also proved by decreasing the initial setting time of the 3DCP mixtures in setting time tests.

3. The printing tests indicate that the nanostructured silica tends to benefit the 3DCP buildability but negatively affects the printing quality correlated to material pumpability. These trends are consistent with the effects of the nanostructured silica on the static yield stress and dynamic yield stress in the rheological tests.
4. By comparing different failure criteria, it shows that for all nanostructured-modified 3DCP cementitious materials, the static yield stress from rheological tests can only quantitively predict the failure caused by gravity-induced vertical stress. Thus, printing tests are still essential to evaluate the printing performance of nanostructured-silica-modified cementitious materials.
5. The results of SEM show that the hydration product of CH is reacted with nanostructured silica and converted into C-S-H due to the pozzolanic reaction. However, heavy carbonation tends to appear with the increasing dosage of nanostructured silica.

In summary, this paper studies the effects of nanostructured silica on rheological properties, hydration properties, microstructural properties, and printing performances of cementitious materials in 3D printing. Based on test results, this paper reveals that nanostructured silica tends to affect the 3DCP buildability positively but negatively affects the printing quality, which is consistent with the effect of nanostructured silica on rheological properties. Thus, the rheological tests are effective in qualitatively evaluating the printing performance, and the printing test method is still essential to further quantitatively determine the 3DCP performance of nanostructured-silica-modified cementitious materials.

Author Contributions: Methodology, Z.L.; formal analysis, Z.L.; Investigation, Z.L. and M.L.; writing—original draft preparation, Z.L. and M.L.; writing—review and editing: M.J.T. and M.L.; supervision, M.J.T. and T.N.W.; Resources, G.S.J.M. and H.K.; project administration: M.L., G.S.J.M. and H.K. All authors have read and agreed to the published version of the manuscript.

Funding: This research is supported by the National Research Foundation, Singapore, Prime Minister's Office, Singapore, under its Medium-Sized Centre funding scheme, Singapore Centre for 3D Printing, and EVONIK (SEA) PTE. LTD.

Data Availability Statement: Not applicable.

Conflicts of Interest: The authors declare no conflict of interest.

References

1. Seol, Y.J.; Kang, H.W.; Lee, S.J.; Atala, A.; Yoo, J.J. Bioprinting technology and its applications. *Eur. J. Cardiothorac. Surg.* **2014**, *46*, 342–348. [CrossRef] [PubMed]
2. Tian, X.; Wu, L.; Gu, D.; Yuan, S.; Zhao, Y.; Li, X.; Ouyang, L.; Song, B.; Gao, T.; He, J.; et al. Roadmap for Additive Manufacturing: Toward Intellectualization and Industrialization. *Chin. J. Mech. Eng. Addit. Manuf. Front.* **2022**, *1*, 100014. [CrossRef]
3. Burger, J.; Lloret-Fritschi, E.; Scotto, F.; Demoulin, T.; Gebhard, L.; Mata-Falcón, J.; Gramazio, F.; Kohler, M.; Flatt, R.J. Eggshell: Ultra-Thin Three-Dimensional Printed Formwork for Concrete Structures. *3d Print. Addit. Manuf.* **2020**, *7*, 48–59. [CrossRef]
4. Jipa, A.; Reiter, L.; Flatt, R.J.; Dillenburger, B. Environmental stress cracking of 3D-printed polymers exposed to concrete. *Addit. Manuf.* **2022**, *58*, 103026. [CrossRef]
5. Labonnote, N.; Rønnquist, A.; Manum, B.; Rüther, P. Additive construction: State-of-the-art, challenges and opportunities. *Autom. Constr.* **2016**, *72*, 347–366. [CrossRef]
6. Ma, G.; Wang, L. A critical review of preparation design and workability measurement of concrete material for largescale 3D printing. *Front. Struct. Civ. Eng.* **2017**, *12*, 382–400. [CrossRef]
7. Mechtcherine, V.; Bos, F.P.; Perrot, A.; da Silva, W.R.L.; Nerella, V.N.; Fataei, S.; Wolfs, R.J.M.; Sonebi, M.; Roussel, N. Extrusion-based additive manufacturing with cement-based materials—Production steps, processes, and their underlying physics: A review. *Cem. Concr. Res.* **2020**, *132*, 106037. [CrossRef]
8. Liu, Z.; Li, M.; Tay, Y.W.D.; Weng, Y.; Wong, T.N.; Tan, M.J. Rotation nozzle and numerical simulation of mass distribution at corners in 3D cementitious material printing. *Addit. Manuf.* **2020**, *34*, 101190. [CrossRef]
9. de Soto, B.G.; Agustí-Juan, I.; Hunhevicz, J.; Joss, S.; Graser, K.; Habert, G.; Adey, B.T. Productivity of digital fabrication in construction: Cost and time analysis of a robotically built wall. *Autom. Constr.* **2018**, *92*, 297–311. [CrossRef]
10. Paul, S.C.; Tay, Y.W.D.; Panda, B.; Tan, M.J. Fresh and hardened properties of 3D printable cementitious materials for building and construction. *Arch. Civ. Mech. Eng.* **2018**, *18*, 311–319. [CrossRef]

11. De Schutter, G.; Lesage, K.; Mechtcherine, V.; Nerella, V.N.; Habert, G.; Agusti-Juan, I. Vision of 3D printing with concrete—Technical, economic and environmental potentials. *Cem. Concr. Res.* **2018**, *112*, 25–36. [CrossRef]
12. Buswell, R.A.; Soar, R.C.; Gibb, A.G.F.; Thorpe, A. Freeform Construction: Mega-scale Rapid Manufacturing for construction. *Autom. Constr.* **2007**, *16*, 224–231. [CrossRef]
13. Suiker, A.S.J.; Wolfs, R.J.M.; Lucas, S.M.; Salet, T.A.M. Elastic buckling and plastic collapse during 3D concrete printing. *Cem. Concr. Res.* **2020**, *135*, 106016. [CrossRef]
14. Weng, Y.; Li, M.; Tan, M.J.; Qian, S. Design 3D printing cementitious materials via Fuller Thompson theory and Marson-Percy model. *Constr. Build. Mater.* **2018**, *163*, 600–610. [CrossRef]
15. Kruger, J.; Zeranka, S.; van Zijl, G. An ab initio approach for thixotropy characterisation of (nanoparticle-infused) 3D printable concrete. *Constr. Build. Mater.* **2019**, *224*, 372–386. [CrossRef]
16. Weng, Y.; Li, M.; Zhang, D.; Tan, M.J.; Qian, S. Investigation of interlayer adhesion of 3D printable cementitious material from the aspect of printing process. *Cem. Concr. Res.* **2021**, *143*, 106386. [CrossRef]
17. Ramakrishnan, S.; Kanagasuntharam, S.; Sanjayan, J. In-line activation of cementitious materials for 3D concrete printing. *Cem. Concr. Compos.* **2022**, *131*, 104598. [CrossRef]
18. Neville, A.M. *Properties of Concrete*; Longman: London, UK, 1995; Volume 4.
19. Kruger, J.; Zeranka, S.; van Zijl, G. A rheology-based quasi-static shape retention model for digitally fabricated concrete. *Constr. Build. Mater.* **2020**, *254*, 119241. [CrossRef]
20. Jiang, Q.; Liu, Q.; Wu, S.; Zheng, H.; Sun, W. Modification effect of nanosilica and polypropylene fiber for extrusion-based 3D printing concrete: Printability and mechanical anisotropy. *Addit. Manuf.* **2022**, *56*, 102944. [CrossRef]
21. Mendoza Reales, O.A.; Duda, P.; Silva, E.C.C.M.; Paiva, M.D.M.; Filho, R.D.T. Nanosilica particles as structural buildup agents for 3D printing with Portland cement pastes. *Constr. Build. Mater.* **2019**, *219*, 91–100. [CrossRef]
22. Lavergne, F.; Belhadi, R.; Carriat, J.; Ben Fraj, A. Effect of nano-silica particles on the hydration, the rheology and the strength development of a blended cement paste. *Cem. Concr. Compos.* **2019**, *95*, 42–55. [CrossRef]
23. Mohammed, A.; Rafiq, S.; Mahmood, W.; Noaman, R.; Al-Darkazali, H.; Ghafor, K.; Qadir, W. Microstructure characterizations, thermal properties, yield stress, plastic viscosity and compression strength of cement paste modified with nanosilica. *J. Mater. Res. Technol.* **2020**, *9*, 10941–10956. [CrossRef]
24. Balapour, M.; Joshaghani, A.; Althoey, F. Nano-SiO_2 contribution to mechanical, durability, fresh and microstructural characteristics of concrete: A review. *Constr. Build. Mater.* **2018**, *181*, 27–41. [CrossRef]
25. Vipulanandan, C.; Mohammed, A. Smart Cement Compressive Piezoresistive, Stress-Strain, and Strength Behavior with Nanosilica Modification. *J. Test. Eval.* **2019**, *47*, 1479–1501. [CrossRef]
26. Rahimzadeh, C.Y.; Salih, A.; Barzinjy, A.A. Systematic Multiscale Models to Predict the Compressive Strength of Cement Paste as a Function of Microsilica and Nanosilica Contents, Water/Cement Ratio, and Curing Ages. *Sustainability* **2022**, *14*, 1723. [CrossRef]
27. Abdalla, A.A.; Salih Mohammed, A.; Rafiq, S.; Noaman, R.; Sarwar Qadir, W.; Ghafor, K.; Al-Darkazali, H.; Fairs, R. Microstructure, chemical compositions, and soft computing models to evaluate the influence of silicon dioxide and calcium oxide on the compressive strength of cement mortar modified with cement kiln dust. *Constr. Build. Mater.* **2022**, *341*, 127668. [CrossRef]
28. Abdalla, A.; Salih, A. Microstructure and chemical characterizations with soft computing models to evaluate the influence of calcium oxide and silicon dioxide in the fly ash and cement kiln dust on the compressive strength of cement mortar. *Resour. Conserv. Recycl. Adv.* **2022**, *15*, 200090. [CrossRef]
29. Bos, F.P.; Kruger, P.J.; Lucas, S.S.; van Zijl, G.P.A.G. Juxtaposing fresh material characterisation methods for buildability assessment of 3D printable cementitious mortars. *Cem. Concr. Compos.* **2021**, *120*, 104024. [CrossRef]
30. Lu, B.; Weng, Y.; Li, M.; Qian, Y.; Leong, K.F.; Tan, M.J.; Qian, S. A systematical review of 3D printable cementitious materials. *Construction and Building Materials* **2019**, *207*, 477–490. [CrossRef]
31. Ma, S.; Qian, Y.; Kawashima, S. Experimental and modeling study on the non-linear structural build-up of fresh cement pastes incorporating viscosity modifying admixtures. *Cem. Concr. Res.* **2018**, *108*, 1–9. [CrossRef]
32. Roussel, N. Rheological requirements for printable concretes. *Cem. Concr. Res.* **2018**, *112*, 76–85. [CrossRef]
33. Qian, Y. *Characterization of Structural Rebuilding and Shear Migration in Cementitious Materials in Consideration of Thixotropy*; Columbia University: New York, NY, USA, 2017.
34. *ASTM-C191*; Standard Test Methods for Time of Setting of Hydraulic Cement by Vicat Needle. American Society for Tesing and Materials: West Conshohocken, PA, USA, 2014. [CrossRef]
35. Yang, H.; Monasterio, M.; Zheng, D.; Cui, H.; Tang, W.; Bao, X.; Chen, X. Effects of nano silica on the properties of cement-based materials: A comprehensive review. *Constr. Build. Mater.* **2021**, *282*, 122715. [CrossRef]
36. Leemann, A.; Winnefeld, F. The effect of viscosity modifying agents on mortar and concrete. *Cem. Concr. Compos.* **2007**, *29*, 341–349. [CrossRef]
37. Roussel, N. A thixotropy model for fresh fluid concretes: Theory, validation and applications. *Cem. Concr. Res.* **2006**, *36*, 1797–1806. [CrossRef]
38. Sikora, P.; Chung, S.-Y.; Liard, M.; Lootens, D.; Dorn, T.; Kamm, P.H.; Stephan, D.; Abd Elrahman, M. The effects of nanosilica on the fresh and hardened properties of 3D printable mortars. *Constr. Build. Mater.* **2021**, *281*, 122574. [CrossRef]

39. Kruger, J.; Zeranka, S.; van Zijl, G. 3D concrete printing: A lower bound analytical model for buildability performance quantification. *Autom. Constr.* **2019**, *106*, 102904. [CrossRef]
40. Alexandridis, A.; Gardner, N. Mechanical behaviour of fresh concrete. *Cem. Concr. Res.* **1981**, *11*, 323–339. [CrossRef]
41. Suiker, A.S.J. Mechanical performance of wall structures in 3D printing processes: Theory, design tools and experiments. *Int. J. Mech. Sci.* **2018**, *137*, 145–170. [CrossRef]
42. Li, W.; Shaikh, F.U.A.; Wang, L.; Lu, Y.; Wang, B.; Jiang, C.; Su, Y. Experimental study on shear property and rheological characteristic of superfine cement grouts with nano-SiO_2 addition. *Constr. Build. Mater.* **2019**, *228*, 117046. [CrossRef]